Fermilab Library
0 1160 0034203 4

SISSA ISAS

Transition in the X-ray light curve of the AM Her system V834 Cen (E1405–451): 1985 – 1986 EXOSAT observations

Rita M. Sambruna[1]

SISSA/ISAS, Via Beirut 2-4, 34014 Trieste, Italy (38028::rita)

Arvind N. Parmar

SSD, European Space Agency, ESTEC, Postbus 229, 2200 AG Noordwijk, The Netherlands
(aparmar@astro.estec.esa.nl)

Lucio Chiappetti

IFCTR-CNR, via Bassini 15, I-20133 Milano, Italy (lucio@ifctr.mi.cnr.it)
Milan, Ist. Fis. Cosmica

Laura Maraschi

Dipartimento di Fisica, via Dodecaneso 33, 16146 Genova, Italy (astmiu::maraschi)
Genoa U.

Aldo Treves

SISSA/ISAS, Via Beirut 2-4, 34014 Trieste, Italy (38028::treves)

NAME | ID No. | M.S.
RETURN TO FERMILAB LIBRARY

SISSA REF 164/93/A

ACCEPTED:

THE ASTROPHYSICAL JOURNAL

[1]Present address: Space Telescope Science Institute, 3700 San Martin Dr., Baltimore, MD 21218 (sambruna@stsci.edu)

ABSTRACT

We analyze the EXOSAT observations of the AM Her system V834 Cen (E1405–451), taken in 1985 March and 1986 August. Archival UV data, simultaneous with the 1986 observations, are also considered. The soft X-ray light curve has a double humped structure, with total eclipse at $\phi \sim 0.0$. It differs significantly from that observed with EXOSAT in 1984. The soft X-ray emission can be described as a blackbody of temperature around 10 – 30 eV, with column density consistent with the interstellar values ($5 \times 10^{19} - 1.0 \times 10^{20}$ cm^{-2}). The hard X-ray emission is nearly sinusoidally modulated with a dip at $\phi \sim 0.0$. This component is consistent with thermal bremsstrahlung emission, with rather high column densitites ($\sim 10^{22}$ cm^{-2}). There is indication for absorption variable with orbital phase. At both epochs, evidence for an iron emission feature at $\sim$ 7.0 keV and with high equivalent widths ($\sim$ 0.8 – 2 keV) is found. The results are discussed in terms of a scenario of the source suggested by the optical and polarization light curves.

Subject Headings: AM Her stars – individual: X-ray – spectra: X-ray – light curves.

1. Introduction

V834 Cen (E1405–451) is a widely studied AM Her (e.g. Tapia 1982; Mason et al. 1983; Nousek & Pravdo 1983; Bailey et al. 1983; Maraschi et al. 1984; Rosen, Mason, & Cordova 1987; Takalo & Nousek 1988). The magnetic field strength, determined both from photospheric Zeeman features and cyclotron emission lines, is $(30.5 \pm 0.5) \times 10^6$ G (Ferrario et al. 1992), a somewhat larger value than the previous estimates of $\sim 10 - 20 \times 10^6$ G (Maraschi et al. 1984; Schwope & Beuermann 1990; Puchnarewicz et al. 1990). Some parameters of the system, taken from the literature, are summarized in Table 1.

The optical light curve of V834 Cen is characterized by the presence of a minimum at orbital phase $\phi \sim 0.0$ (Bailey et al. 1983; Mason et al. 1983), implying that the magnetic field axis points in our direction at this phase. The strong linear polarization pulse at $\phi \sim 0.5$ indicates that the angle between the accreting field lines and the observer becomes maximum. The accreting pole always remains in view during the orbital motion, because the circular polarization curve mantains the same (positive) sign (Bailey et al. 1983; Cropper 1989). The accretion stream intercepts the line of sight at $\phi \sim 0.0$, causing a dip in the circularly polarized light at this phase (Cropper 1989). Support for this view is also provided by the fact that $i + \beta < 90°$ (King & Williams 1985).

The shape of the optical curve was observed to change radically in data taken several months apart, from double to single humped (Cropper, Menzies, & Tapia 1986; Cropper 1989). Ferrario & Wickramasinghe (1990) modelled the cyclotron emission in the optical assuming an extended emission region, at small distances from the magnetic dipole (Ferrario et al. 1992). Because of projection and cyclotron beaming effects, variation in the position and elongation of the arc, due to a variable accretion rate, are supposed to be the cause of the observed pattern change.

V834 Cen was observed in X-rays by the HEAO 1 and *Einstein* satellites in the 0.1 – 2.8 keV energy range (Jensen, Nousek, & Nugent 1982) and by EXOSAT on three occasions (1984 March, 1985 August, and 1986 March) in the range 0.1 – 10 keV. We studied the 1984 EXOSAT data in a previous paper, together with simultaneous optical, IR, and UV observations (Sambruna et al. 1991 = S91).

The EXOSAT observations are of particular interest because they allow a spectral and temporal study of the source emission simultaneously in two energy decades (0.1 –10 keV). In the case of the 1984 data, the spectrum could be fitted with two distinct components, a low energy blackbody with a well determined temperature (14 – 16 eV) and absorption consistent with the galactic values (5 – 6 $\times 10^{19}$ cm^{-2}), and a high energy bremsstrahlung component, with kT $\geq$ 1.0 keV and high, orbital phase dependent absorption ($\sim 10^{23}$ cm^{-2}). The soft X-ray light curve showed a double eclipse structure at $\phi \sim 0.0$, coincident with the optical minimum and with a maximum in the hard X-ray light curve.

In a preliminary analysis of the 1985 and 1986 EXOSAT light curves, Osborne, Cropper, & Cristiani (1987) found a radically different soft X-ray light curve compared to 1984. Similar behavior is also observed in the simultaneous optical data.

In this paper we reconsider the 1985 and 1986 EXOSAT data and present a detailed analysis. In addition to the light curves, we study the average and phase resolved ME spectra. The results of the temporal and spectral analysis are described in sections 2.2 and 2.3, respectively. UV archival data, quasi-simultaneous to the 1986 EXOSAT observations, are also considered (section 3). Our findings are discussed in section 4.

2. X-ray data. Analysis and Results

2.1. The observations

The data were obtained with the Low Energy (LE) and Medium Energy (ME) instruments on board the EXOSAT satellite (White & Peacock 1988 and references therein), operating in the 0.02 – 2.5 keV and 1 – 50 keV energy ranges, respectively. A log of the observations is given in Table 2. The analysis procedure is similar to that adopted in S91, and we refer to this paper for details.

The LE images, taken with the 3000 Lexan (3LX) and the aluminum-parylene (Al-P) filters at both epochs, were analyzed using the X-ray image analysis package XIMAGE (Giommi & Tagliaferri 1991). The count rates were extracted in a box of optimum size 50 pixels (1 pixel = 4 arcsec) centered on the source position and corrected for vignetting, dead time, and point spread function (Table 2). At both epochs the observations with the 3LX filter are longer than those in the Al-P, covering 4.5 and 11 times the orbital cycle of the system (orbital period = 101.5 min) for 1985 and 1986, respectively. The Al-P observations have a duration less than one cycle, yielding count rates at lower significance (4 and 3 σ, respectively).

In the ME instrument only the data from the Argon chamber are used. The background was obtained in both observations using array swap data. The last 18400 s of the 1986 exposure were discarded because of the unstable background. The source was detected in the energy range 2 – 10 keV. The count rates extracted in this range are reported in Table 2.

The 1986 count rate is higher than in 1985 in LE by a factor 1.7 and in ME by a factor 2. If the 1984 observation is considered (Table 1A of S91), it is found that this observation

is intermediate in ME intensity between the 1986 and 1985 ones, but has the highest count rate in LE.[1]

2.2. Temporal analysis

2.2.1. The LE light curves

Only the data taken with the 3LX filter, for which a longer time coverage was available (Table 2), were used. The data were folded over the orbital period using the ephemeris of Cropper, Menzies, & Tapia (1986) as in S91, where phase zero refers to the minimum of the optical light curve.

The folded data are shown in Figure 1, where, for comparison, we also present the archival 1984 LE light curve in the 3LX filter. The overall shape of the 1985 and 1986 light curves is characterized by a broad minimum at $\phi \sim 0.3$ and 0.5, respectively, and by a total eclipse at $\phi \sim 0.1$. In the case of the 1985 observation an additional eclipse is present at $\phi \sim 0.0$. This feature is also observed in the 1984 data.

The gross shape of the soft X-ray light curve changes substantially from 1984 to 1986. In the former observation the overall shape of the light curve is rather complex, with a minimum around $\phi = 0.3$, followed by bump-like features. At the latter epoch the shape appears symmetric, with a broad minimum centered at $\phi \sim 0.5$. The optical light curves, taken simultaneously to the EXOSAT observations, are also observed to change in shape, from asymmetric to double humped (S91; Osborne, Cropper, & Cristiani 1987).

---

[1]The 3LX intensity reported in S91 is misprinted. The count rate should read 0.6072 $\pm$ 0.0089 counts s^{-1} (instead of 0.6972).

V834 Cen is one of the few AM Her systems in which drastic long term changes in the soft X-ray light curves have been observed. Similar behavior has been reported for AM Her, QQ Vul (E2003+225), and MR Ser (Heise et al. 1985; Osborne et al. 1987; Angelini, Osborne, & Stella 1990). QQ Vul, in particular, shows both "complex" and "simple" modes rather similar to the 1984 and 1986 light curves of V834 Cen.

2.2.2. The ME light curves

The 1985 and 1986 ME light curves, accumulated in 2 – 10 keV and corrected for dead time, were folded with the above ephemeris. The results are shown in Figure 2 together with the archival 1984 data. A common feature of the three light curves is a dip between $\phi \sim 0.9 - 0.1$, almost coincident with the eclipses in the corresponding LE data.

The 1986 light curve, for which the signal to noise ratio is higher, appears sinusoidally modulated. The hypothesis of constant emission can be rejected, the fit with a constant curve yielding $\chi^2 = 126$ for 30 bins, corresponding to an acceptance probability $P_{\chi^2} < 10^{-9}$. In contrast, the 1985 light curve shows less modulation, with $\chi^2 = 46/30$ and $P_{\chi^2} \sim 3\%$. Similar values are found for the 1984 light curve. The limited statistics do not allow further comments about the shape of the light curves.

2.3. Spectral analysis

2.3.1. The soft component

Spectral information for the soft component can be derived from the LE count rates in the way described in S91. Assuming that the LE flux may be modelled with a blackbody spectrum, we can reproduce the ratio of the 3LX and Al-P count rates for the 1985 and

1986 observations in the (N_H, T_s) space, where N_H is the column density in cm^{-2} and T_s the blackbody temperature in eV. Figure 3 shows the 1σ (68%) contour for the 1986 data, for which the quasi-simultaneous UV observations (see section 3) allowed a better determination of the spectral parameters. The UV flux, reproduced as a solid line in Figure 3, leads to the shaded area, which constrains N_H in the range $\sim 5 \times 10^{19} - 1.5 \times 10^{20}$ cm^{-2} and $T_s \sim 10.5 - 35.0$ eV. The temperature range is consistent with the values derived for the 1984 LE data (15 $\pm$ 1 eV) and the absorption is consistent with the interstellar values (S91).

Fixing N_H at 5 $\times 10^{19}$ cm^{-2}, derived from the 1984 observations, gives for 1986 T_s = 15 – 29 eV. The blackbody flux, corrected for absorption, is thus in the range (0.68 – 1.02) $\times 10^{-11}$ ergs cm^{-2} s^{-1}, a factor $\gtrsim$ 10 lower than observed in 1984, $\sim 34.0 \times 10^{-11}$ ergs cm^{-2} s^{-1} (S91). For the 1985 contour the above fixed absorption gives T_s = 6 – 30 eV which leads to a flux in the range (0.37 – 0.87) $\times 10^{-11}$ ergs cm^{-2} s^{-1}.

2.3.2. The hard component

The ME spectra were analyzed using the XSPEC fitting program (Shafer *et al.* 1991). As in S91, we fitted the data with absorbed bremsstrahlung and power law spectral models. The results are shown for both the observations in Table 3a, where we list the fit temperature T_h (in keV), the photon index α_{ph}, the column density N_H (in cm^{-2}), and the reduced χ^2 per degrees of freedom (χ^2_ν/dof). Uncertainties are quoted at 90% confidence ($\Delta\chi^2 = 4.6$). Also reported in Table 3a is the flux measured in the 2 – 6 keV range and corrected for absorption. The fact that the two spectral models used give equivalent fits can be attributed to the limited energy range where the signal was detected.

The parameters of the fits are poorly determined, especially for the 1985 observation. For completeness we reported in Table 3a the nominal best fits for T_h (minimum χ^2 values).

We can only constrain the temperature to be > 10 keV. An absorbing column density $\sim 10^{22}$ cm^{-2} is obtained in both cases. This value is rather high compared to the interstellar column density, $\sim 10^{19} - 10^{20}$ cm^{-2}, but is one order of magnitude lower than the value measured for the 1984 spectrum ($N_H \sim 3 - 4 \times 10^{23}$ cm^{-2}). No significant differences are found for the shape of the continuum among the three observations.

Table 3a shows that the fits with the bremsstrahlung and power law models to the 1985 and 1986 spectra are not satisfactory, with reduced χ^2 corresponding to acceptance probabilities of 8.8% and $\lesssim$ 2.0%, respectively. From Figures 4a and 4b, where the observed spectra and the residuals from the bremsstrahlung fits are shown, it is apparent an excess of photons around 7 keV in both observations, which may be evidence for the presence of an emission Fe feature. We model this feature by adding a narrow (FWHM width, σ_L, fixed at 0.1 keV) gaussian line to the above models. The results of the fits are reported in Table 4, where the energy center line, E_L, and its equivalent width, EW, are given together with the continuum parameters. An F-test shows that the improvement in the χ^2 is significant, $\sim$ 97% and 95% for 1985 and 1986, respectively. In both spectra the center energy is constrained in a rather broad range, 6.5 – 7.4 keV. The 1984 ME spectrum does not show evidence for an emission feature around 7.0 keV.

The EW found for the 1986 data is consistent with values found for other AM Her systems (Rothschild et al. 1981; Ishida et al. 1989; Kallman et al. 1993).

2.3.3. Phase-resolved ME spectra

We have accumulated ME spectra on selected phase intervals, chosen from the folded light curves in Figure 2, with the criterion that the emission level in each interval should be nearly constant. For both epochs we identified at least three ranges, corresponding to high, low, and intermediate emission states. The spectra accumulated in these intervals

were fitted with the same spectral models as above. Due to the poorer statistics, we only considered the continuum models without the inclusion of the gaussian line. In Table 5 we report the results of these fits.

The temperature and photon index are poorly determined and do not vary with the phase in both observations. A weak variation of the absorption with the phase is indicated in the 1986 observation, a result similar to that found for the 1984 data (S91). In the high state, the column density could not be kept as a free parameter of the fit and was thus fixed at discrete values. The minimum χ^2 was found for $N_H = 5 \times 10^{19}$ cm^{-2}.

3. UV observations

IUE observed V834 Cen the day after the EXOSAT observations in 1986 (Table 2). A set of five spectra (2 SWP and 3 LWP) were available from the IUE archive. No significant variability was found among the spectra taken in each of the two cameras, which were therefore summed producing the combined spectrum shown in Figure 5.

For fitting purposes the continuum was measured by averaging the flux in 50 Å intervals in selected line free regions. The errors in each bin are the combination of statistical and systematic uncertainties. The spectrum was fitted with a power law model, $F_\lambda \propto \lambda^{-\alpha_{UV}}$, reddened with the extinction curve of Seaton (1979). The fit results are summarized in Table 3b, where the best fit and 90% confidence error of the spectral slope and of the extinction, A_V, are reported. To better constrain the α_{UV} range we also performed a fit with A_V fixed at the best fit value 0.75 (Table 3b). The flux at 1300 Å, corrected for the absorption, is $F_{1300} = 1.28 \times 10^{-14}$ ergs cm^{-2} s^{-1} Å^{-1}. This flux was used in section 2.3.1 to better contrain the blackbody temperature.

The 1986 UV spectrum is close in slope and flux to the high state measured 1982

(Nousek & Pravdo 1983) and in 1983 (Maraschi et al. 1984). In 1984 a flatter slope ($\alpha_{UV} \sim$ 1.5) and a somewhat higher flux (3.0 $\times 10^{-14}$ ergs cm^{-2} s^{-1} Å^{-1}) were observed. Usual emission lines, with intensities similar to previous observations, are also present (Figure 5).

4. Discussion

EXOSAT observations of the AM Her system V834 Cen, during 1985 and 1986, are presented. Our principal findings are:

1) The light curves in 0.1 – 2.0 keV energy range were found to have a different shape with respect to a previous set of data, taken in 1984. In 1986 it is simple and symmetric, with a large minimum at $\phi \sim 0.5$, while a rather asymmetric shape was observed in 1984. A permanent feature during all observations is the presence of total eclipses around $\phi \sim 0.0$.

2) The LE data suggest a blackbody temperature of $\sim$ 20 eV.

3) The ME light curves appear sinusoidally modulated, with a dip at $\phi \sim 0.0$. The modulation is more clearly seen in the 1986 data.

4) The hard X-ray spectrum is consistent with a bremsstrahlung of $T_h \sim 10 - 100$ keV, with some evidence that the absorption varies with orbital phase.

5) In both 1985 and 1986, but not in 1984, there is evidence for an Fe K emission line at energies $\sim$ 7.0 keV, with large EW ($\sim$ 0.8 – 2 keV).

4.1. Emission regions

We estimated the areas of the regions emitting the soft blackbody (A_{bb}) and hard bremsstrahlung (A_{bremss}) X-rays for the 1984 and 1986 EXOSAT observations, for which the higher quality data were obtained, using our measured fluxes and temperatures reported

above. For A_{bremss} we followed Beuermann (1989), who calculates this area in terms of the bremsstrahlung emission measure, the shock height, and the density, assuming a constant cooling rate. From his eq. (6), we found $A_{bremss} \lesssim 2.0 \times 10^{14}$ and $\sim 1.5 \times 10^{12}$ cm^2 for the 1984 and 1986 observations, respectively (for a distance of 100 pc; S91). The specific luminosities L/f (where f is the fractional accretion area) are $\gtrsim 2.0 \times 10^{36}$ and $\sim 7.0 \times 10^{37}$ ergs s^{-1} for the two epochs, respectively, both corresponding to the bremsstrahlung dominated regime of Lamb & Masters (1979). For the blackbody emitting regions we found $A_{bb} \sim 4 \times 10^{15}$ and 5×10^{13} cm^2, thus decreasing by a factor ~ 100 from 1984 to 1986. The values of the X-ray emitting areas for V834 Cen are comparable to those inferred by Beuermann (1989) for other four AM Her systems, and in both observations $A_{bremss} < A_{bb}$, as predicted by the standard theory.

Considering in addition the region emitting cyclotron, Beuermann (1989) showed that $A_{bremss} < A_{cyc}$, while A_{bb} is intermediate. This is reminiscent of the core-halo model (Liebert & Stockman 1985; Stockman & Lubenow 1987), where a bremsstrahlung dominated core is surrounded by a cyclotron dominated halo, with the accretion rate decreasing from the core to the halo. In the case of the 1984 observation, for which IR data were available (S91), the cyclotron emission area A_{cyc} could be calculated. We found $A_{cyc} \sim 10^{14}$ cm^2, only marginally consistent with the values listed by Beuermann (1989) for other four objects, and close to the area emitting the soft blackbody. The specific luminosity for the cyclotron component is 3×10^{35} ergs s^{-1}, lower than that reported above for the bremsstrahlung region, suggesting that at this epoch a core-halo structure may be present. Because of the lack of IR measurements, we can not comment about A_{cyc} at the latest epochs.

4.2. The light curves

We observed two different types of soft X-ray light curves in V834 Cen, a "simple mode" in 1986 and a "complex mode" in 1984 (Figure 1). Similar transitions were also observed in QQ Vul, a system expected to have the same geometry as V834 Cen (Osborne *et al.* 1987).

As in QQ Vul, the simple 1986 light curve can be understood in the accretion geometry of the system as deduced from the optical data (section 1). If matter accretes uniformly over a circular emission region, as in the simple radial models (e.g. Imamura & Durisen 1987), projection area effects are sufficient to explain the observed shape. In this context, the broad minimum at $\phi = 0.5$ in Figure 1 is due to the fact that the we see only a small fraction of the emitting region at this phase. The eclipse at $\phi = 0.0$, where a peak of the blackbody emission is expected, can be attributed to intervening matter, which we identify with the accretion funnel (see section 1). From King & Williams (1985) and using the parameters of Table 1, the narrow ($\Delta\phi = 0.02$) width of the eclipse implies a stream radius D $\sim 2.5 \times 10^7$ cm, which is large enough to occult substantially the blackbody area (see above).

The "complex mode" observed in 1984 can not be easily explained in the context of a uniform, radial accretion. The observed asymmetric shape probably requires a changing geometry, in which projection area effects become less important. A comparison with the cyclotron light curves may help. As discussed above, these were observed to change from double humped to single humped. This was modelled as an effect of variation in position and elongation of an arc-like emission region, at some distance from the dipole axis (Ferrario & Wickramasinghe 1990). In particular, the single humped shape observed for the optical light curve, simultaneous to the 1984 LE complex mode, would be related to a maximum width and elongation toward the magnetic equator of the arc. The fact that the cyclotron

and blackbody regions may be spatially coincident (see above) can support the possibility that soft X-rays originate in a similar region. Variable accretion rate profiles along the arc (see e.g. Stockman 1989) can easily reproduce the bump-like features observed in the LE light curve in 1984.

Note also that the source exhibits a strong soft excess at this epoch (S91). A similar effect was observed during the "reverse mode" of AM Her (Heise et al. 1985), which was explained by requiring accretion at a second pole. In V834 Cen, the first evidence for a second active region, coming into view at $\phi \sim 0.1$, was inferred from polarization data (Cropper 1989; Ferrario & Wickramasinghe 1990). It is thus possible that the extra emission in the 1984 LE data between $\phi = 0.0 - 0.1$ comes from a second region, which would also contribute to the ME light curve at these phases (Figure 2).

We thus witness two different accretion conditions in 1984 and 1986. In the latter case, simple radial models are good descriptions of the data. In contrast, in 1984 this simple picture probably does not apply and it is possible that an additional active region is present.

The ME light curve observed in 1986 shows a sinusoidal modulation with a dip starting at $\phi \sim 0.0$. This shape is less clear in the two earlier observations. The coincidence of the dip with the eclipse in the LE data points toward a common origin in the accretion stream. The column density required for the dip, $\sim 10^{22}$ cm^{-2}, is high enough to absorb radiation at lower energy. Concerning the observed modulation, we can think of two possible causes: (1) the emitting area undergoes substantial obscuration by the limb of the white dwarf during the orbital motion, or (2) X-ray beaming is present, due to absorbing matter inhomogeneously distributed around the accreting area. A modelling of (1) was done by Imamura & Durisen (1983) for a range of inclination i and colatitude β angles. The computed hard X-ray light curves would have the shape observed for $i \sim 60°$ and $\beta \sim 30° - 60°$, which are both too large (Table 1). Hypothesis (2) is supported by the

analysis of the phase resolved ME spectra (section 2.3.3), in which an indication for the dependence of the accretion column density on orbital phase is present, with maximum and minimum N_H at $\phi \sim 0.5$ and 0.0, respectively. A similar phase dependence of N_H was observed for the 1984 light curve, with higher values (S91), and suggests that the hard X-ray emitting region is embedded in a ring of cool matter with a column density of $\sim 10^{22} - 10^{23}$ cm^{-2}. The possible presence of cool gas surrounding the accretion region was first derived from the study of cyclotron emission lines (Wickramasinghe, Tuohy, & Visvanathan 1987), and is consistent with the core-halo model discussed above.

4.3. Iron line

In the ME spectra evidence is found for an iron emission feature, with fitted center energy $\sim$ 7.0 keV and large EW. An iron line was previously observed in higher sensitivity data of AM Her itself (Rothschild et al. 1981), EF Eri (White 1981), and BY Cam (Ishida et al. 1989; Kallman et al. 1993).

Swank, Fabian, & Ross (1984) proposed a model to account for the observed properties of the line observed in the HEAO 1 spectrum of AM Her ($E_L = 6.5 \pm 0.15$ keV, EW = 0.8 ± 0.1 keV). The line was modelled as a mixture of a thermal component at 6.9 keV, produced by the postshock gas, and a fluorescence component at 6.4 keV, originating from the white dwarf surface and the accretion column. However, higher quality GINGA and BBXRT observations of BY Cam showed that this model is probably incorrect. In the latter data an iron line was observed at $6.6^{+0.09}_{-0.07}$ keV with EW = 500 ± 148 eV (Kallman et al. 1993) and could not be described by the combination of the 6.4 and 6.9 keV components. Instead, a blend of two lines at 6.6 and 6.9 keV was consistent with the data, thus indicating the prevalence of the thermal contribution. This kind of picture seems consistent with our observations of V834 Cen, but higher resolution X-ray spectroscopy is obviously needed for

a more quantitative discussion.

We are grateful to Elena Pian for her help with the analysis of the UV data and to Joe Pesce for a careful reading of the manuscript. Julian Osborne is acknowledged for his friendly collaboration. R.M.S. thanks SISSA for financial support.

Table 1

Parameters of E1405-451

Parameter		Ref.
Orbital period	101.5 min	1
White dwarf mass	(0.63 – 0.86) $M_\odot$	2
White dwarf radius	(5.8 – 8.0) $\times 10^8$ cm	2
Secondary mass	0.21 $M_\odot$	2
Secondary radius	1.4 $\times 10^{10}$ cm	2
Inclination i	45° - 60°	3
Magnetic colatitude β	10° - 35°	3
Polar field strength	30.5 $\pm$ 0.5 MG	3
Distance	$\geq$ 70 pc	4
Galactic absorption	5 $\times 10^{19}$ – 1.0 $\times 10^{20}$ cm^{-2}	5

References: 1=Mason et al. (1983); 2=Rosen, Mason, & Cordova (1987); 3=Ferrario et al. (1992); 4=Puchnarewicz et al. (1990); 5= from Paresce (1984).

Table 2

Journal of 1985 – 1986 Observations

a. X-ray observations

Instrument	Start Date	Start Time (UT)	Exposure Time (s)	Count rate (cts s^{-1})
LE + 3000 Lexan	1985 Aug 2	05:31	27358	0.224 ± 0.004
LE + Aluminum-Parylene		11:49	2852	0.025 ± 0.006
ME		05:29	35460	0.673 ± 0.028 [a]
LE + 3000 Lexan	1986 Mar 5	11:01	67172	0.377 ± 0.003
LE + Aluminum-Parylene	1986 Mar 6	09:57	5148	0.034 ± 0.011
ME	1986 Mar 5	10:54	75310	1.372 ± 0.026 [a]

b. UV observations

Camera/Image Number	Start Date	Start Time	Exposure (s)
SWP 27857	1986 Mar 7	06:33	2880
SWP 27858		09:14	2880
LWP 7747		04:50	5820
LWP 7748		07:26	5820
LWP 7749		10:07	1800

Notes to Table 1:

(a): Counts s^{-1} $half^{-1}$ in the 2 – 10 keV range

Table 3

Summary of Spectral Fits

a. ME spectra

Model	$\alpha_{ph}^{(a)}$	$T_h^{(a)}$ (keV)	$N_H^{(a,b)}$ ($\times 10^{22}$ cm^{-2})	χ^2_ν/dof	Flux$_{2-6keV}$ (10^{-12} ergs cm^{-2} s^{-1})
			1985		
Bremsstrahlung	···	100.7 (< 143.6)	0.77 (< 2.51)	1.4/25	6.08
Power Law	$1.29^{+0.62}_{-0.43}$	···	0.84 (< 3.07)	1.4/25	6.08
			1986		
Bremsstrahlung	···	$25.4^{+49.5}_{-11.5}$	$0.58^{+0.58}_{-0.53}$	1.6/32	11.5
Power Law	1.52 ± 0.20	···	$0.87^{+0.76}_{-0.71}$	1.7/32	11.4

b. 1986 UV spectrum

Model	α_{UV}	A_V	χ^2_ν/dof	Flux$_{1300}$ (10^{-14} ergs cm^{-2} s^{-1} Å^{-1})
Power law	$2.05^{+0.55}_{-0.35}$	$0.75^{+0.45}_{-0.35}$	3.4/20	1.28
	2.09 ± 0.13	0.75	3.4/20	···

Notes to Table 2:

(a): Best fit values and 90% confidence intervals.

(b): Morrison & McCammon (1983) cross section.

Table 4

ME spectra: Continuum + Gaussian Line [a]

Model	$\alpha_{ph}^{(a)}$	$T_h^{(a)}$ (keV)	$N_H^{(a,b)}$ ($\times 10^{22}$ cm^{-2})	E_L (keV)	EW (keV)	χ^2_ν/dof
			a. 1985			
Bremsstrahlung	···	$5.6^{+51.1}_{-0.50}$	$2.2^{+2.8}_{-2.0}$	$6.86^{+0.41}_{-0.33}$	$2.45^{+2.33}_{-1.42}$	0.92/23
Power Law	$2.37^{+1.27}_{-0.96}$	···	$3.4^{+3.8}_{-2.8}$	$6.87^{+0.41}_{-0.34}$	$2.32^{+1.94}_{-1.31}$	0.94/23
			b. **1986**			
Bremsstrahlung	···	$11.0^{+12.9}_{-4.20}$	$1.0^{+0.7}_{-0.6}$	7.05 ± 0.40	$0.775^{+0.595}_{-0.450}$	1.33/30
Power Law	$1.80^{+0.32}_{-0.28}$	···	$1.5^{+1.0}_{-0.8}$	$7.02^{+0.43}_{-0.51}$	$0.686^{+0.534}_{-0.451}$	1.44/30

Notes to Table 3:

(a): σ_L fixed at 0.1 keV

(b): Best fit values and 90% confidence intervals

(c): Morrison & McCammon (1983) cross section

REFERENCES

Angelini, L., Osborne, J.P, & Stella, L. 1990, MNRAS 245, 652

Bailey, J., Axon, D.J., Hough, J.H., Watts, D.J., Giles, A.B., & Greenhill, J.G. 1983, MNRAS 205, 1P

Beuermann, K. 1989, in "Polarized Radiation of Circumstellar Origin", Eds. G.V.Coyne et al., Vatican Observatory – Vatican City State, p. 125

Cropper, M. 1989, MNRAS 236, 935

Cropper, M., Menzies, J.W., & Tapia, S. 1986, MNRAS 218, 201

Ferrario, L. & Wickramasinghe, D.T. 1990, ApJ 357, 582

Ferrario, L., Wickramasinghe, D.T., Bailey, J., Hough, J.H., & Tuohy, I.R. 1992, MNRAS 256, 252

Giommi, P. & Tagliaferri, G. 1991, XIMAGE User's Guide, Version 1.8, (Noordwijk: ESA)

Jensen, K.A., Nousek, J.A., & Nugent, J.J. 1982, ApJ 261, 625

Heise, J., Brinkman, A.C., Gronenschild, E., Watson, M., King, A.R., Stella, L., & Kieboom, K. 1985, A&A 148, L14

Ishida, M., Silber, A., Bradt, H.V., Remillard, R.A., Makishima, K., & Ohashi, T. 1989, ApJ 367, 270

Kallmann, T. et al. 1993, ApJ 411, 869

King, A.R. & Williams, G.A. 1985, MNRAS 215, 1P

Imamura, J.N. & Durisen, R.H. 1983, ApJ 268, 291

Lamb, D.Q. & Masters, A.R. 1979, ApJ 234, L117

Liebert, J. & Stockman, H.S. 1985, in Cataclysmic Variables and Low-Mass X-ray Binaries, eds D.Q. Lamb & J. Patterson (Dordreicht:Reidel), 151

Maraschi, L. et al. 1984, ApJ 285, 214

Mason, K.O. et al. 1983, ApJ 264, 575

Morrison, R. & McCammon, D. 1983, ApJ 270, 119

Nousek, J.A. & Pravdo, S.H. 1983, ApJ 266, L39

Osborne, J., Beuermann, K., Charles, P., Maraschi, L., Mukai, K., & Treves, A. 1987, ApJ 315, L123

Osborne, J.P., Cropper, M., & Cristiani, S. 1987, Astroph. Sp. Sci. 130, 643

Paresce, F. 1984, AJ 96, 1022

Puchnarewicz, E.M., Mason, K.O., Murdin, P.G., & Wickramasinghe, D.T. 1990, MNRAS 244, 20P

Rosen, S.R., Mason, K.O., & Cordova, F.A. 1987, MNRAS 224, 987

Rothschild, R.E. et al. 1981, ApJ 250, 723

Sambruna, R.M. et al. 1991, ApJ 374, 744 (S91)

Schwope, A.D. & Beuermann, K. 1990, A&A 238, 173

Seaton, M. J. 1979, MNRAS, 187, 73P

Shafer, R.A., Haberl, F., Arnaud, K.A., & Tennant, A.F. 1991, XSPEC User's Guide, Version 2 (ESA TM – 09)

Stockman, H.S. 1989, in "Polarized Radiation of Circumstellar Origin", Eds. G.V.Coyne et al., Vatican Observatory – Vatican City State, p. 237

Stockman, H.S. & Lubenow, A.F. 1987, Astr.Spa.Sci. 131, 607

Swank, J.H., Fabian, A.C., & Ross, R.R. 1984, ApJ 280, 734

Takalo, L.O. & Nousek, J.A. 1988, ApJ 327, 328

Tapia, S. 1982, IAU Circ., No. 3685

White, N.E. 1981, ApJ 244, L85

White, N.E. & Peacock, A. 1988, The EXOSAT Observatory, in "X-Ray Astronomy with EXOSAT", Eds. Pallavicini, R. & White, N.E., Italian Astronomical Society, Firenze, p.1.

Wickramasinghe, D.T., Tuohy, I.R., & Visvanathan, N. 1987, ApJ 318, 326

This manuscript was prepared with the AAS LaTeX macros v3.0.

Fig. 1.— The LE light curves of V834 Cen in 1984, 1985, and 1986. Data are folded with the ephemeris of Cropper, Menzies, & Tapia (1986), and normalized by dividing by the average intensity.

Fig. 2.— The ME light curves of V834 Cen in 1984, 1985, and 1986 (see Figure 1).

Fig. 3.— Determination of the blackbody spectral parameters for the 1986 observation. The light shaded area surrounded by thin contours represent the region allowed (within 1σ uncertainties) by the ratio of the count rates in the 3LX and Al-P filters (see S91 for a description of the method). The thick solid line corresponds to the measured UV flux. The dark shaded area is the region in the parameter space allowed by the X-ray and UV measurements. This figure can be compared directly to Fig. 4 of S91; note however that the temperature range here is larger, and that the better statistics in 1984 allowed S91 to use the 3σ errors).

Fig. 4.— The 1985 and 1986 ME spectra. Upper panels: observed spectra and bremsstrahlung folded model. Lower panels: the residuals of the fit.

Fig. 5.— The 1986 UV spectrum.

FIG. 1

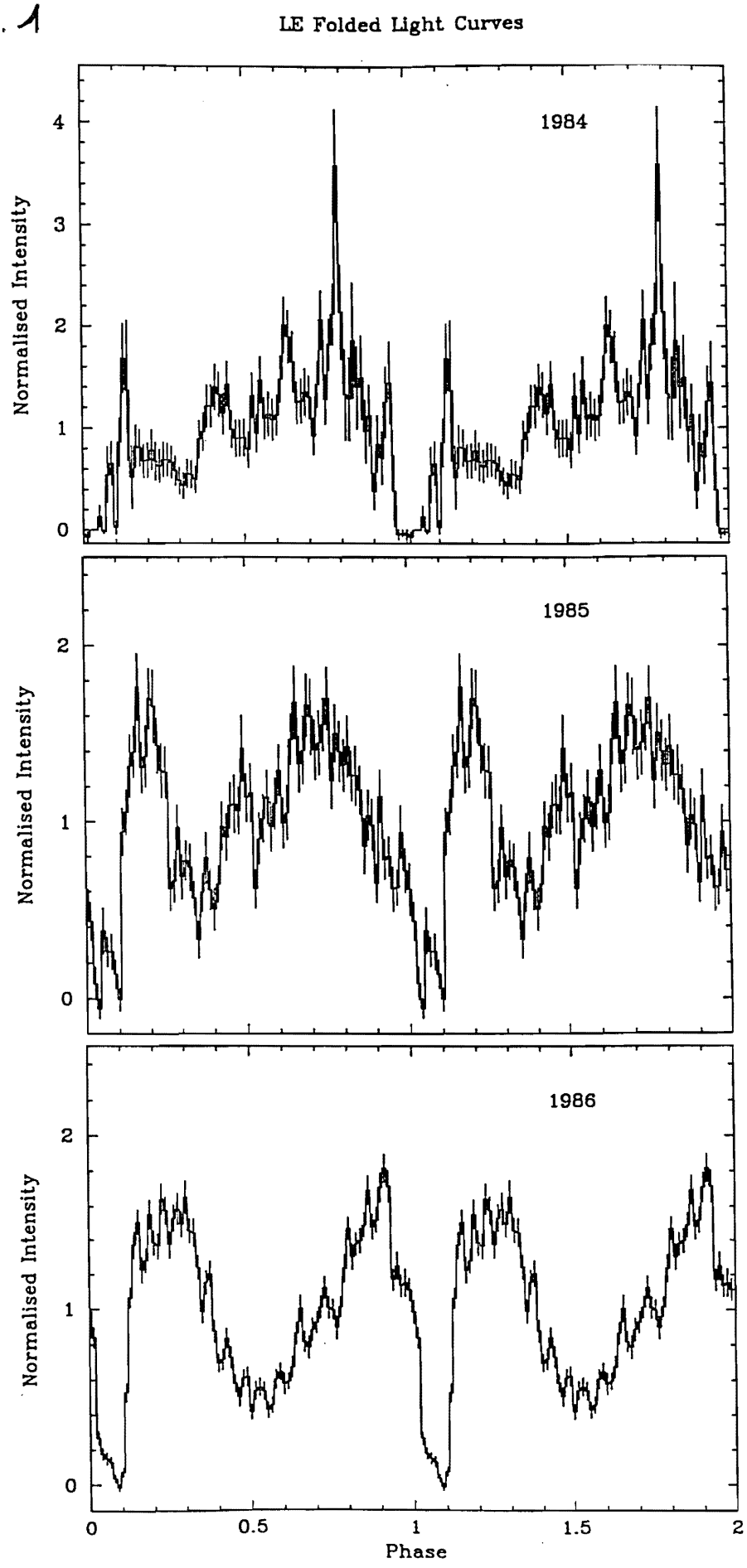
LE Folded Light Curves
1984
1985
1986
Normalised Intensity
Normalised Intensity
Normalised Intensity
0
1
2
3
4
0
1
2
0
1
2
0
0.5
1
1.5
2
Phase

FIG. 2

ME Folded Light Curves

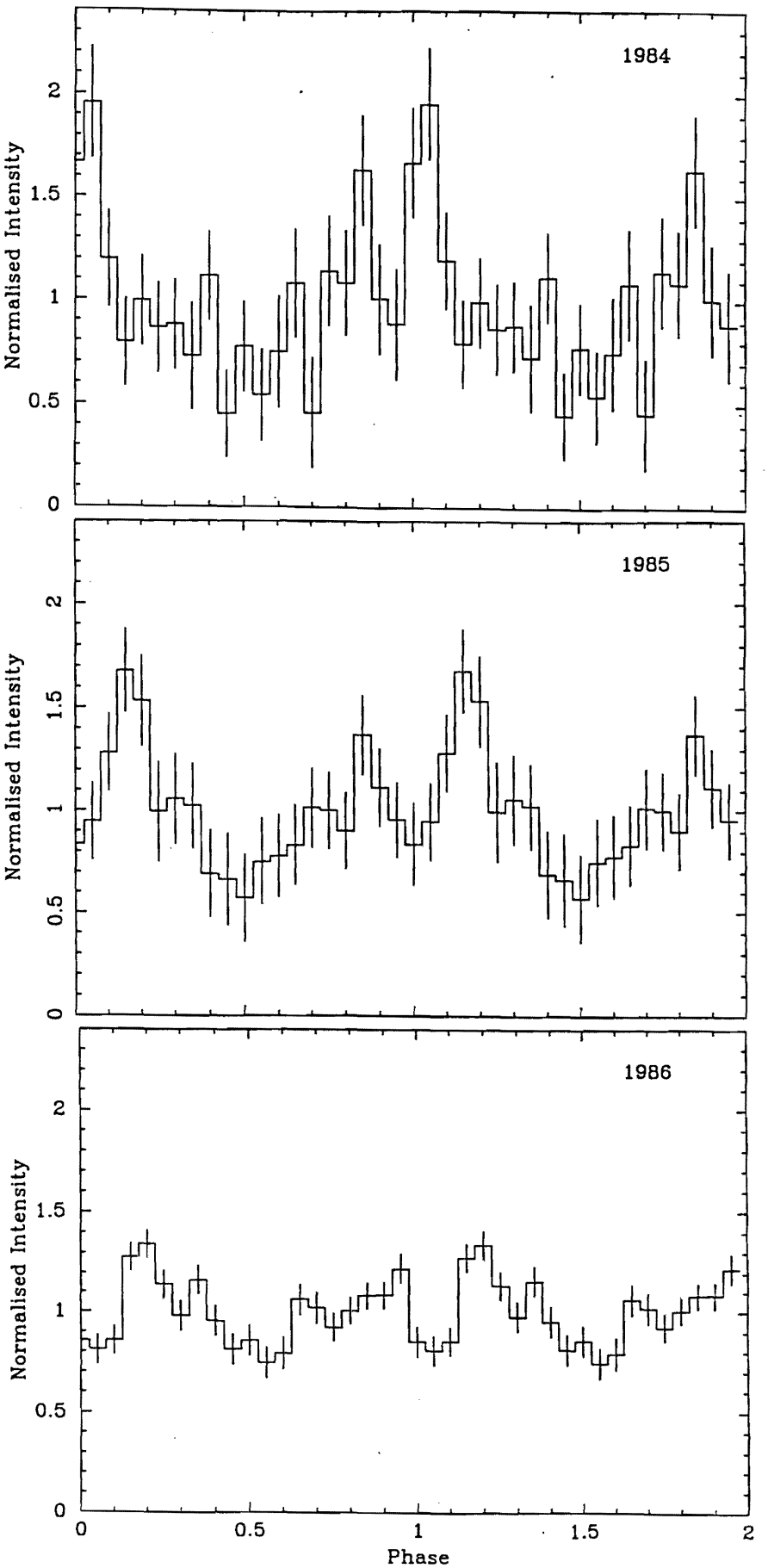

FIG. 3

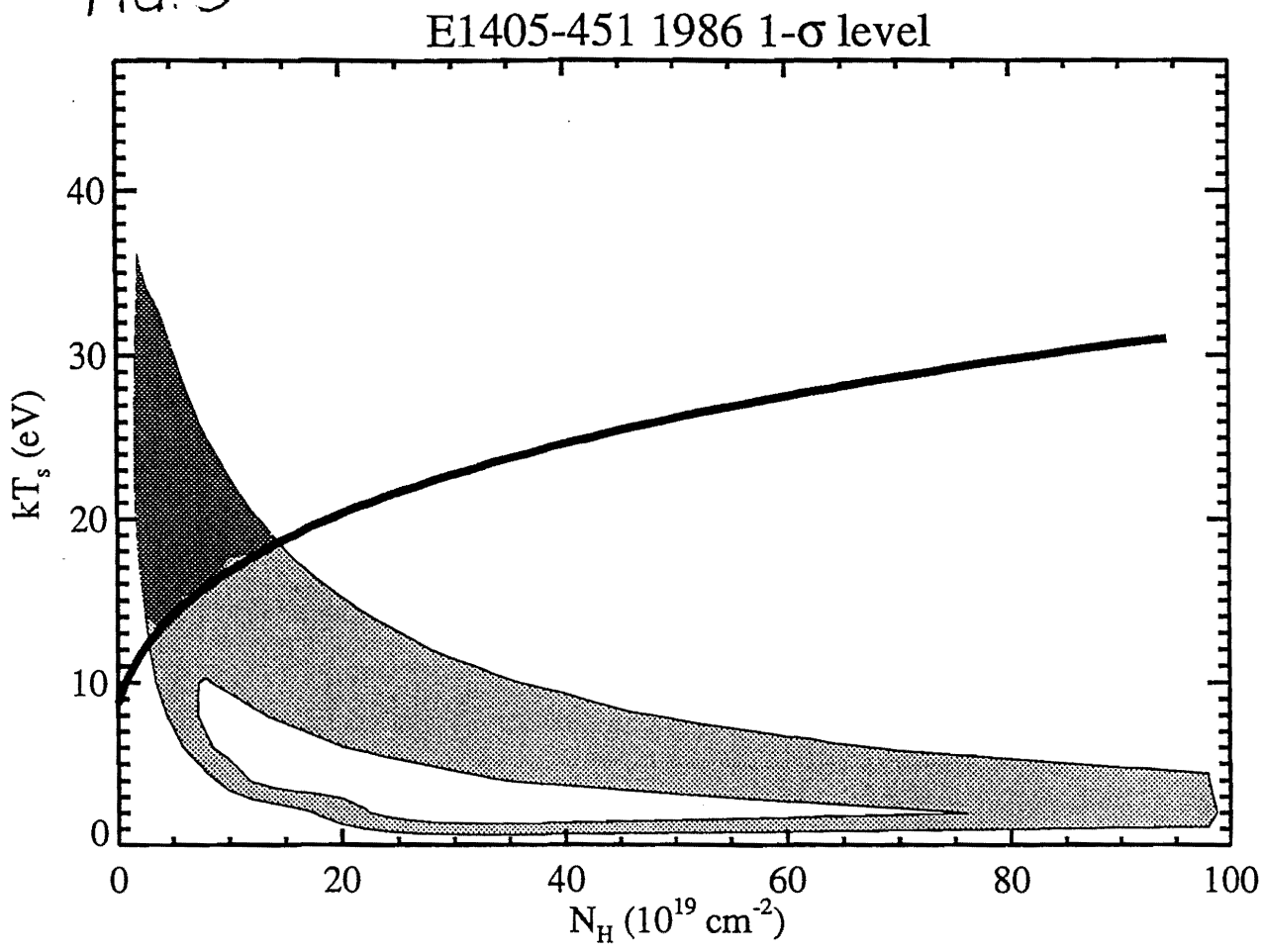
E1405-451 1986 1-σ level
kT$_s$ (eV)
0
10
20
30
40
0
20
40
60
80
100
N$_H$ (10^{19} cm^{-2})

FIG. 4

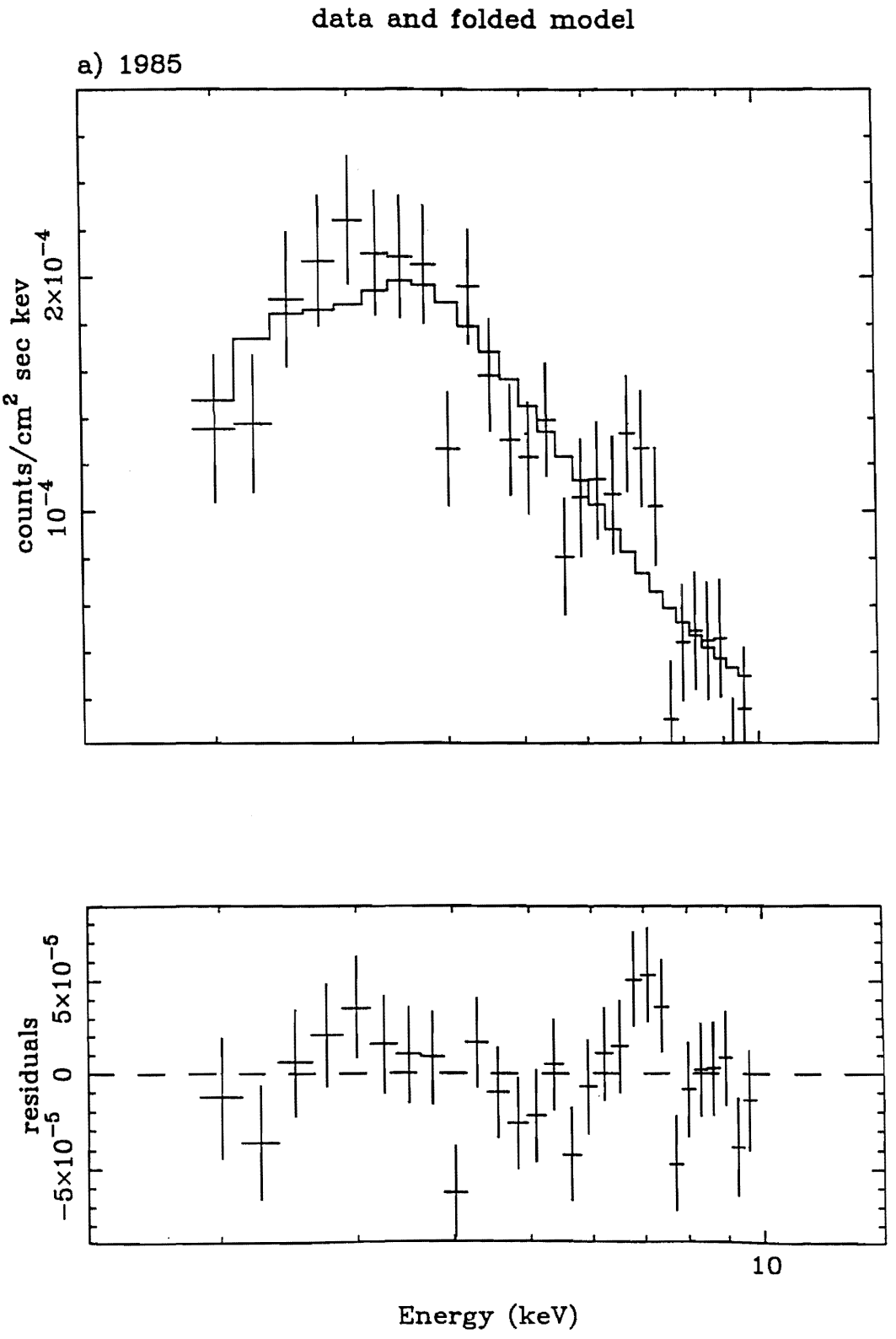
data and folded model
a) 1985
counts/cm^2 sec kev
2×10^{-4}
10^{-4}
residuals
5×10^{-5}
0
-5×10^{-5}
10
Energy (keV)

FIG. 4

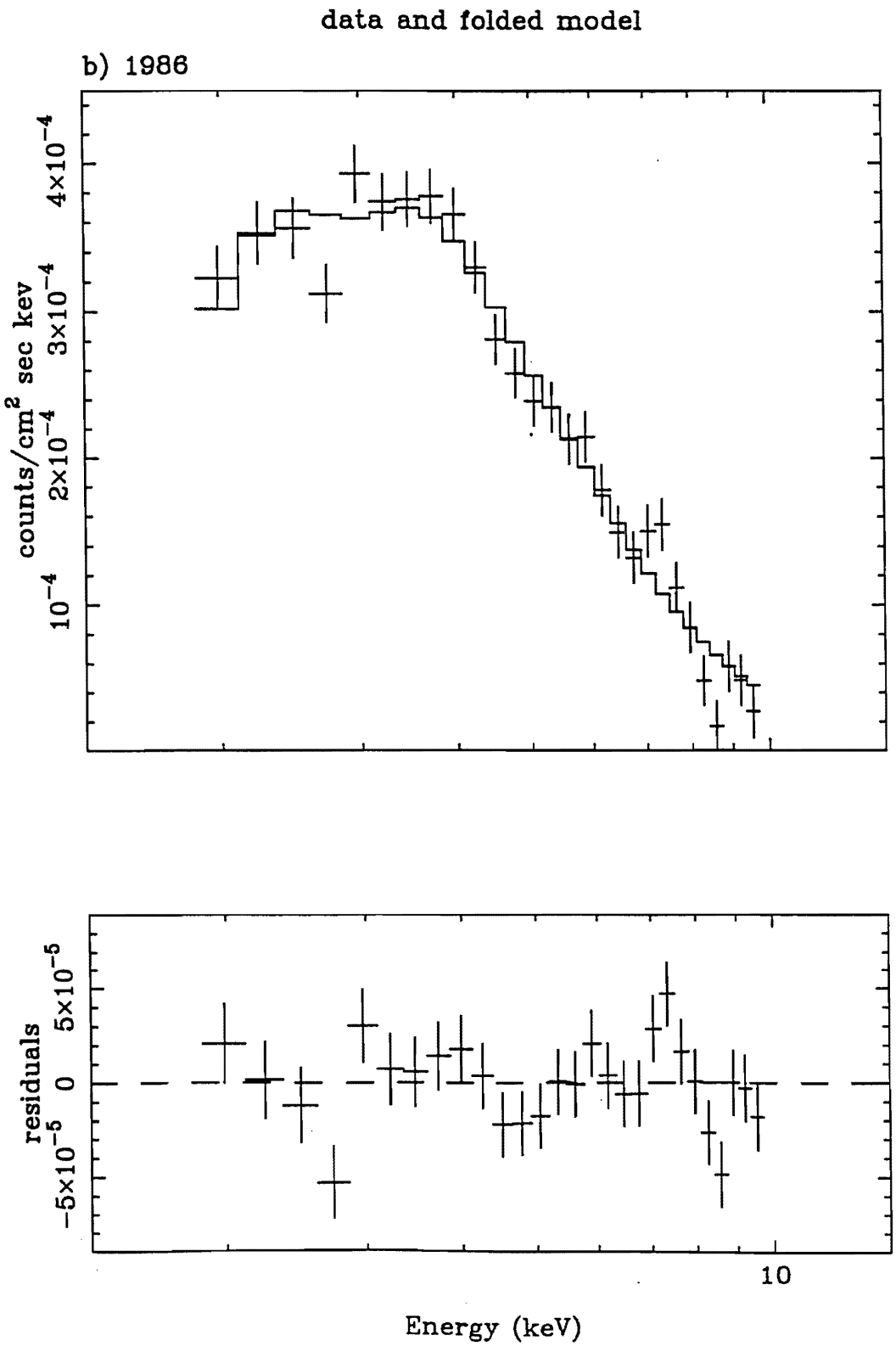
data and folded model
b) 1986
counts/cm^2 sec kev
4×10^{-4}
3×10^{-4}
2×10^{-4}
10^{-4}
residuals
5×10^{-5}
0
-5×10^{-5}
10
Energy (keV)

Fig. 5

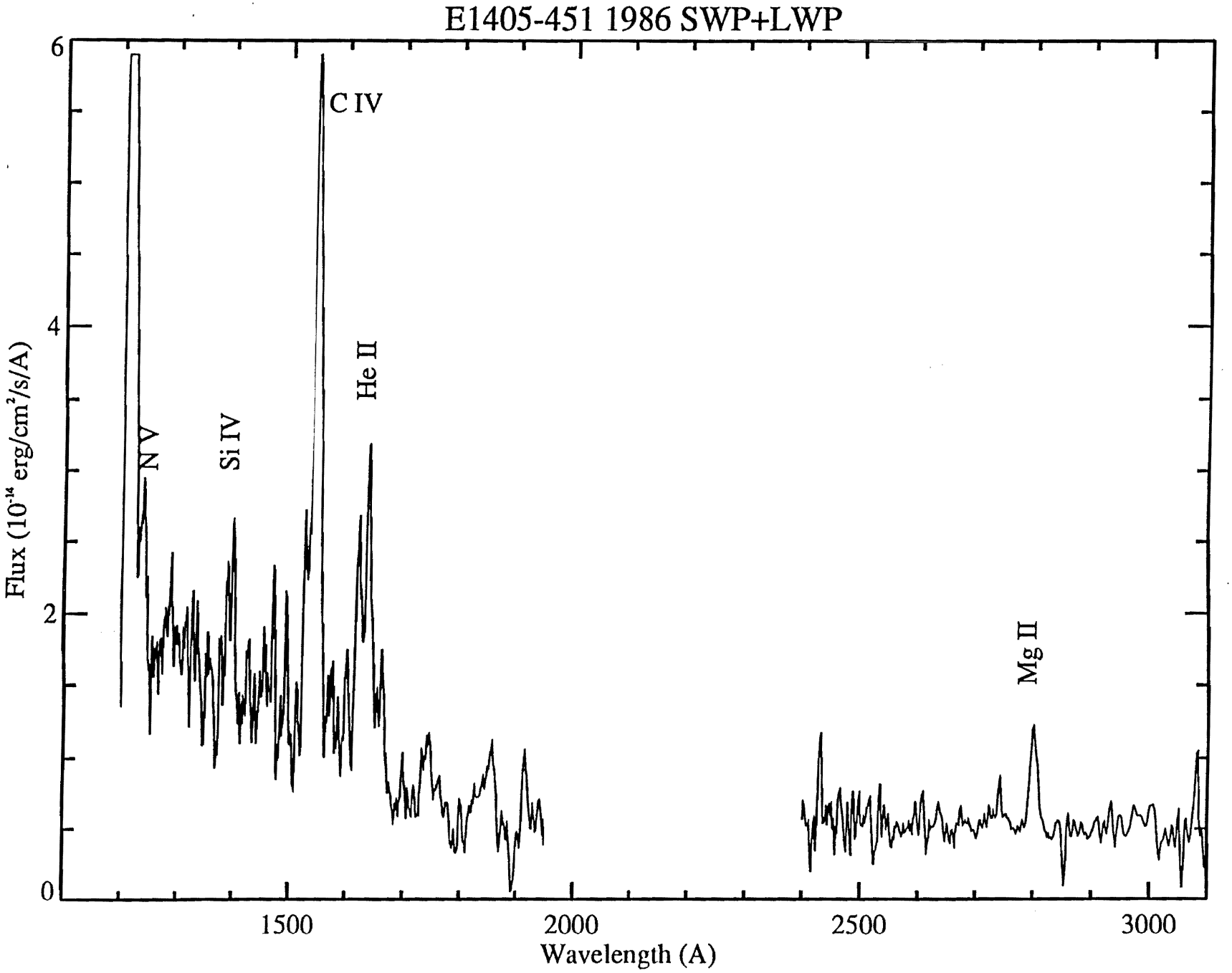
E1405-451 1986 SWP+LWP
Flux (10^{-14} erg/cm^2/s/A)
Wavelength (A)
N V
Si IV
C IV
He II
Mg II
0
2
4
6
1500
2000
2500
3000